P Selected for a Viewpoint in *Physics*

PHYSICAL REVIEW LETTERS

Cavity Induced Shift and Narrowing of the Positronium Lyman-α Transition

D. B. Cassidy,[1] M. W. J. Bromley,[2] L. C. Cota,[2] T. H. Hisakado,[1] H. W. K. Tom,[1] and A. P. Mills, Jr.[1]

[1]*Department of Physics and Astronomy, University of California, Riverside, California 92521-0413, USA*
[2]*Department of Physics and Computational Science Research Center, San Diego State University,
San Diego, California 92182-1233, USA*

We report experiments in which the line shape of the Lyman-alpha (1S-2P) transition was measured for positronium (Ps) atoms both inside and outside a porous silica target. The energy interval ΔE for confined atoms was observed to be larger than that of free Ps by 1.26 ± 0.06 meV. A configuration interaction calculation yields results that are consistent with our ~ 5 nm sample, and suggests that ΔE decreases dramatically for larger cavity diameters. The linewidth of the transition, (0.066 ± 0.004) nm (FWHM), is about half of what one would expect for free Ps at room temperature due to the Dicke line narrowing effect of confinement. Such measurements can be used to determine void sizes in porous films and Ps dynamics therein, and elimination of the Doppler spread of atoms in a porous film could be useful for the efficient excitation of a Ps gas.

PACS numbers: 36.10.Dr, 31.15.ag, 34.80.Nz, 37.30.+i

The thought experiment in which an atom is placed inside an impenetrable cavity is an appealing one that has a long history [1]. As well as providing an interesting model [2], this type of arrangement is directly relevant to real physical systems, such as atoms and molecules trapped in fullerenes [3] or in high pressure environments [4]. The constrained motion of confined atoms allows for recoil and Doppler free spectroscopy [5], which is useful, for example, in the production of an optical lattice atomic clock [6]. Advances in the production of engineered porous materials [7], for which there are a multitude of applications [8], have provided a convenient way to produce and study confined atoms, including positronium (Ps) [9].

Here we present spectroscopic measurements of Ps [10] confined inside a porous film. The atoms were created by irradiating a silica target with positrons that capture electrons in the bulk material and form Ps, which subsequently diffuses into the pores and becomes trapped therein. Our data exhibit a large shift in the 1S-2P transition energy and a narrowing of the line shape due to confinement of Ps in the porous silica matrix. Atomic line shifts typically arise due to perturbations of the internal wave function, with the center of mass (c.m.) motion being essentially classical. For Ps in a small cavity, however, the direct interaction of the electron and positron with the wall potential leads to both a mixed c.m. and relative coordinate wave function, and a Ps lineshift orders of magnitude larger than would be expected for heavier atoms under similar conditions.

Laser spectroscopy of Ps in small pores can be used to determine pore sizes (even with closed pore structures), measure Ps cooling and diffusion rates, and efficiently produce excited state atoms for use in the formation of antihydrogen beams [11]. We note that recently laser spectroscopy of O_2 gas in porous Al_2O_3 was performed [12] and line broadening due to wall collisions was observed, which could be used to measure pore sizes in samples with open pore structures.

Our experiments were performed using an accumulator [13] that delivers sub-ns pulses containing $\sim 2 \times 10^7$ positrons to a porous silica target in an axial magnetic field of ~ 0.3 T. Annihilation radiation was observed via single-shot lifetime spectra [14]. When ground-state Ps is excited to a 2P state and then photoionized, relatively long-lived triplet atoms are converted into free electron-positron pairs. Typically the liberated positrons will rapidly annihilate, which leads to changes in Ps lifetime spectra, as shown in Fig. 1. We analyze such spectra to determine the parameter f_d which is the fraction of the total spectrum in the interval from 50 to 300 ns. Recording the change in f_d as a function of the excitation laser wavelength yields a Ps excitation line shape.

A Q-switched Nd:YAG laser with harmonic generators was used to provide 532 nm and 355 nm light pulses approximately 7 ns wide, full width at half maximum
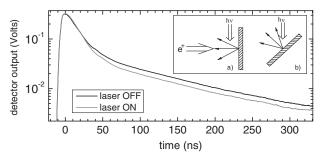

FIG. 1. Single-shot lifetime spectra with and without firing the lasers. The curves are averages of 8 shots each. The inset shows the target (shaded rectangle) and beam orientations (open arrows) for measuring vacuum Ps (a) and Ps while it is still inside the silica target (b). The spectra shown here were taken in configuration (a).

(FWHM). The latter was used to pump a dye laser (LD 489 dye) to produce 486 nm light, which was frequency doubled in a beta barium borate (BBO) crystal to produce 243 nm light. The Gaussian line profile had a width of (0.004 ± 0.0002) nm (FWHM), with a time width of ~4 ns. The diameter of the 243 nm beam was ~3 mm at the target position, and the positron beam diameter was <1 mm. More details concerning the general methodology can be found in Ref. [15].

The silica film used here had an open pore structure, a density of ~1.5 g/cm^3 and a nominal pore diameter of ~5 nm [16]. The target could be irradiated in two configurations, as indicated in Fig. 1. With the laser parallel to the target surface only Ps in vacuum could be excited, whereas when the target was rotated by $\sim45°$ the laser entered the silica, and Ps could be excited while inside the film [17]. This was possible because the time taken for Ps to diffuse out into the vacuum may be of the order of the Ps lifetime in the pore, which in the present case is >50 ns [16].

Figure 2 shows measurements of the $1S$-$2P$ line shape made with the target perpendicular (a) and at $\sim45°$ (b) and (c) to the positron beam axis. Single-shot lifetime spectra were used to determine the parameter $S(\lambda) \equiv (f_{off} - f_{on})/f_{off}$, where $f_{off(on)}$ refers to f_d measured with the lasers off (on). Measurements were made with the lasers fired at the same time as the positron pulse ("prompt") or with a delay of 20 ns ("delayed"). Figure 2(a) shows
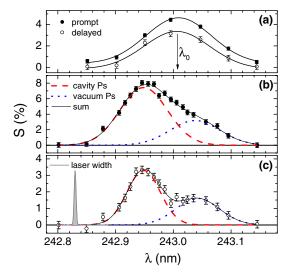

FIG. 2 (color online). Lineshapes measured for Ps in vacuum (a) and with the laser incident on the target material (b) and (c). The lasers were either prompt (filled circles) or delayed (open circles) as explained in the text. The data may be decomposed into two Gaussians, corresponding to Ps inside (dashed lines) and outside (dotted lines) the cavity. The bandwidth of the laser ~0.004 nm is shown in (c), shifted for clarity. Each data point is from a single shot, with uniform error bars determined from the assumption that the chisquare per degree of freedom should be 1 for the fitted curves. A background has been subtracted in (b) and (c) but not in (a).

measurements of vacuum Ps in which we observe a Doppler broadened line shape centered at a mean wavelength $\lambda_0 = (243.008 \pm 0.002)$ nm (vacuum wavelengths are quoted) differing by 0.016 nm from the $1S$-$2P$ wavelength (243.024 ± 0.002) nm, where the error is due to the variation in energy across the $2P$ manifold and possible Zeeman-Stark shifts [18]. The discrepancy is due to uncertainty in the absolute wavelength calibration. The Doppler width, (0.16 ± 0.02) nm, is due to the conversion of the Ps confinement energy to kinetic energy upon ejection from the pores (see Ref. [15]).

A very different situation was observed when the target was rotated so that the laser light passed through the sample. In this case a resonant line was still observed, but it was shifted from the vacuum position. The line shape was also quite asymmetrical, and for the delayed data it is clear that there are two distinct Ps populations, neither of which is centered at the unperturbed $1S$-$2P$ transition wavelength. The measurements can be decomposed into a sum of two Gaussians, as indicated in Figs. 2(b) and 2(c). The shorter wavelength components (dashed lines) centered at $\lambda_b = (242.948 \pm 0.007)$ and $\lambda_c = (242.948 \pm 0.002)$ have FWHM's $\Delta\lambda_b = (0.088 \pm 0.008)$ and $\Delta\lambda_c = (0.061 \pm 0.004)$ nm. The average $1S$-$2P$ interval observed is thus (1.26 ± 0.06) meV more than the unperturbed interval. These lines are due to Ps atoms probed while they are inside the silica film.

The longer wavelength components (dotted lines in Fig. 2) correspond to free Ps in vacuum. These lines are shifted to wavelengths longer than λ_0 [by (0.034 ± 0.018) nm and (0.029 ± 0.006) nm in panels (b) and (c), respectively] because the Ps is, on average, moving towards the laser. The corresponding line widths, (0.092 ± 0.026) and (0.080 ± 0.013) nm, are primarily due to the angular divergence of the nearly monoenergetic Ps [15].

The lowest energy level of a ground-state Ps atom in an infinite spherical potential well of diameter $2R_0$ is $E_0 \approx 750$ meV $\times (1$ nm$/2R_0)^2$ relative to the vacuum [15]. Since the radius of a $2P$ Ps atom is larger than that of a $1S$ atom by ~3 Bohr radii a_0, one would expect the $2P$ energy level to be higher by a factor of order unity times $\Delta E_0 = 6E_0 a_0/R_0$. Thus, in a 5 nm diameter pore with $E_0 \sim 30$ meV, $\Delta E_0 = 3.6$ meV.

A more realistic determination of the cavity shift of the $1S$-$2P$ transition must include not only the perturbation of the center of mass, but also the effect of the external potential on the relative coordinate wave function. We have undertaken *ab initio* calculations of a Ps atom confined in model cavities using the configuration interaction (CI) method. Without the benefit of reducing the two-body problem to an effective one-body problem, these are challenging two-body calculations due to the positron-electron localization [19]. Wave functions built using single particle orbitals about the center of the cavity require the inclusion of high values of angular momenta [20], here $l = 0, \ldots, 12$.

Estimates of the complete basis-set limit were also obtained using extrapolation methods as developed for CI calculations of positronic atoms [21] and helium [22].

The CI method, as applied to the e^+/e^- in a central (atomic) potential problem, has been explored in depth previously [23]. A brief description is given here as it is applied to a cavity. The nonrelativistic Hamiltonian includes, besides the interparticle Coulomb potential, a Woods-Saxon-like cavity potential $V_c(r) = V_0\{1 - [1/(1 + \exp\{(r - R_0)/x_0\})]\}$ where $2V_0$ is the height of the Ps-cavity wall potential located at diameter $2R_0$, r is the electron or positron coordinate, and the potential varies over a length x_0. The CI wave function with total angular momentum, L, and spin S is a linear combination of single particle e^+/e^- orbitals, written as a product of a spherical harmonic and a Laguerre-type radial orbital (LTO). The basis set is built with $N_{\max}$ LTOs per partial wave, up to a maximum angular momentum $L_{\max}$. The LTO exponents were optimized in a calculation of the $^1S^e$ ground state with $L_{\max} = 12$ and $N_{\max} = 10$, with $2R_0 = 3$ nm, $V_0 = 0.5$ eV and $x_0 = 0.0529$ nm.

Computational validations were performed on "free" space positronium ($V_0 = 0$) with $L_{\max} = 12$ and $N_{\max} = 35$ in both $^1S^e$ and $^1P^o$ channels (with 15 925 and 29 400 configurations, respectively). In atomic units, $E(^1S^e) = -0.232\,052$, which lies below that of a previous Gaussian-type orbital calculation ($-0.211\,398$) [19]. After eliminating dipole-inaccessible states that consist of Ps(1S) orbiting $r = 0$ in a p-wave (as positronic atoms also prefer [24]) we obtain $E(^1P^o) = -0.059\,738$, i.e., a transition energy of $\Delta E = 4.689$ eV, which is within 10% of the exact (5.102 eV). Calculations with $L_{\max} = 10$ and 11 were then performed, and an extrapolation to $L_{\max} \rightarrow \infty$ obtained using "method p" of Ref. [21], which resulted in $E(^1S^e) = -0.252\,071$ and $\Delta E = 5.170$ eV. Furthermore, to obtain an estimate of the complete basis-set limit, $N_{\max} = 33$, 34, 35 calculations were performed and extrapolations in both $N_{\max} \rightarrow \infty$ and $L_{\max} \rightarrow \infty$ gave $\Delta E = 5.138$ eV.

Figure 3 shows the calculated change in the transition energy induced by various cavity sizes, relative to the free-space calculation, $\delta\varepsilon(V_0, R_0) = \Delta E(V_0, R_0) - \Delta E(V_0 = 0)$. Since the height of the Ps-cavity potential
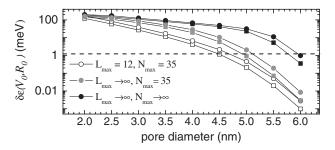

FIG. 3. The change of the Ps $1S$-$2P$ transition energy as a function of the cavity diameter ($2R_0$). Data are given for cavity potential barrier heights, $2V_0 = 1$ eV (squares) and 3 eV (circles). The dashed line indicates the measured shift.

for solid SiO_2 is known to be between 1 and 3 eV [25], the barrier height *per particle* V_0 was chosen to be 0.5 and 1.5 eV. The explicit calculations appear to provide a lower bound on the shift $\delta\varepsilon(V_0, R_0)$, as two estimates of the basis-set limits were also obtained using the aforementioned extrapolation procedures for each V_0 and R_0. Relatively large extrapolated shifts are obtained, however, and even the $L_{\max} \rightarrow \infty$ corrections are likely to be overestimated, as previous studies of "method p" indicate [21]. This is exacerbated by the slow convergence of the shift with respect to both $N_{\max}$ and $L_{\max}$ [26]. From these results, the measured $1S$-$2P$ cavity shift of 1.3 meV therefore corresponds to a cavity diameter of (5.25 ± 0.75) nm.

The sharp change in slope of the calculated cavity $1S$-$2P$ interval at ~ 5 nm diameter appears not to be an artefact of the calculations. Rather, this is a result of the differing diameters of the cavity $1S$ versus $2P$ states. Although their eigenenergies are only slightly changed from the free Ps levels, the wave functions of both the $1S$ and $2P$ cavity states are very different compared to those of free atoms. The $1S$ state, which is deeply bound by the Coulomb interaction, has a c.m. that is strongly concentrated in the middle of the cavity potential (e.g., $\langle r_e \rangle = \langle r_p \rangle \approx 7$ a.u. for $2V_0 = 1$ eV and $2R_0 = 4$ nm), and tends to keep away from the walls. The $2P$ state, due to its angular momentum, surprisingly fills up the cavity (e.g., $\langle r_e \rangle = \langle r_p \rangle \approx 17$ a.u.). This is related to its having an internal energy (-13.6 eV/8) that is comparable to the cavity potential barrier. Thus, the $2P$ c.m. is able to tunnel into the barrier, experiencing more of a perturbation which increases the energy of the $2P$ more than the $1S$ state. For cavity diameters beyond a few times $\langle r_e \rangle$ (i.e., 5 nm) the difference in the behavior of the $1S$ and $2P$ wave functions diminishes abruptly, as does the magnitude of the cavity shift. This effect emerges clearly from the calculations, despite the uncertainty in the absolute values of $\delta\varepsilon(V_0, R_0)$.

We do not expect any significant occupation of excited cavity states for thermalized Ps (that is, Ps that is no longer losing energy by collisions with the walls [15]). Also, the time taken for Ps to thermalize in a cavity of diameter ~ 5 nm is of the order of 10 ns [27]. As a result, the downshifted prompt data [Fig. 2(b)] are almost certainly due to nonthermal Ps that is not all in the cavity ground state, and the downshifted delayed data [Fig. 2(c)] to thermalized Ps that is in the cavity ground state. These lines indicate that ΔE does not depend greatly on whether the ground or first center of mass excited state of the cavity is occupied. We note that, since only stationary states are included, the CI calculation does not address this observation. Neither does it take into account any effects due to van der Waals-type wall interactions [28]. However, based on the shift of optical transitions for atoms held near a wall [29], this effect should be at least an order of magnitude smaller than our observed cavity shift.

Dicke line narrowing [30] results from restraining an atomic center of mass, so that the average velocity during the absorption of a photon is reduced, and thus also the Doppler spread. For any Ps atoms observed *inside* the sample (as evidenced by the downshifted line center) this effect should reduce the Doppler spread to a width much less than the laser bandwidth of ~ 0.004 nm [31]. For a collection of isolated pores with a variation of radii we would expect a corresponding variation in the magnitude of the line center shift, which would produce a broader line. However, as the prompt line is shifted by almost the same amount as the delayed line, but is also wider, this cannot be the only source of broadening in our measurements.

If the pores in our silica film have some short range order then, at thermal energies, Ps therein will be in a pseudo Bloch state in the lowest energy band of the pore structure. The bandwidth of such a structure will be of the order of a few meV, which is the same order of magnitude as the observed width of the thermal Ps line shape. There would not usually be any line broadening associated with this since the crystal momentum k is conserved in an optical transition. The observed broadening may be explained by a combination of (1) the differing widths of the $1S$ versus the $2P$ bands, with the latter being narrower than the former because of the reduced interpore tunneling of the larger diameter $2P$ atoms, and (2) some degree of k nonconservation, due to disorder. These effects will be larger for Ps in the first cavity excited state, giving rise to an even broader linewidth for the nonthermal data, since the bands are more free-particle-like at higher kinetic energies, leading to larger bandwidths.

It would be informative to perform this type of measurement using samples with isolated pores of varying, well defined sizes, allowing a more extensive comparison with calculations. Since the cavity shift can be used to distinguish between Ps inside and outside the sample, if a 1 ns wide laser were used it should be possible to directly measure the Ps emission rate without time of flight or geometrical complications. Similarly, the time dependence of the linewidth could be used to measure the Ps cooling rate. If a sample with a high degree of order were used the linewidth of thermalized Ps might be very narrow; this could facilitate the production of large bursts of excited state atoms with a low power, narrow bandwidth excitation laser, which may be useful for some antihydrogen experiments [11], as the Doppler broadened linewidth of even low temperature Ps is larger than typical laser bandwidths. The ability to perform laser spectroscopy on confined atoms is expected to open up new methods for measuring the properties of porous films, as well as the dynamics of Ps made in such materials.

[1] A. Sommerfeld and H. Welker, Ann. Phys. (Leipzig) **424** 56 (1938).
[2] W. Jaskólski, Phys. Rep. **271**, 1 (1996).
[3] D. S. Bethune, *et al.*, Nature (London) **366**, 123 (1993); K. Komatsu, M. Murata, and Y. Murata, Science **307**, 238 (2005); H. Shinohara, Rep. Prog. Phys. **63**, 843 (2000).
[4] J. M. Lawrence, P. S. Riseborough, and R. D. Parks, Rep. Prog. Phys. **44** 1 (1981).
[5] T. Ido and H. Katori, Phys. Rev. Lett. **91**, 053001 (2003).
[6] M. Takamoto *et al.*, Nature (London) **435**, 321 (2005).
[7] D. Y. Zhao *et al.*, Science **279** 548 (1998).
[8] M. E. Davis, Nature (London) **417**, 813 (2002).
[9] D. B. Cassidy and A. P. Mills, Jr, Nature (London) **449**, 195 (2007).
[10] A. Rich, Rev. Mod. Phys. **53**, 127 (1981).
[11] F. Castelli *et al.*, Phys. Rev. A **78**, 052512 (2008); M. Doser *et al.* (AEGIS collaboration), Journal of Physics Conference Series **199**, 012009 (2010).
[12] T. Svensson and Z. Shen, Appl. Phys. Lett. **96**, 021107 (2010).
[13] D. B. Cassidy *et al.*, Rev. Sci. Instrum. **77**, 073106 (2006).
[14] D. B. Cassidy *et al.*, Appl. Phys. Lett. **88**, 194105 (2006).
[15] D. B. Cassidy *et al.*, Phys. Rev. A **81**, 012715 (2010).
[16] P. Crivelli *et al.*, Phys. Rev. A **81**, 052703 (2010).
[17] Laser irradiation of the silica produced a background effect that was not cumulative and could be subtracted. With different silica films we have observed cumulative laser induced damage that would make experiments of the type we describe here impossible. D. B. Cassidy *et al.*, Phys. Rev. B **75**, 085415 (2007).
[18] S. M. Curry, Phys. Rev. A **7**, 447 (1973).
[19] G. L. Bendazzoli, S. Evangelista, and T. Leininger, Int. J. Quantum Chem. **85**, 118 (2001).
[20] J. Mitroy, M. W. J. Bromley, and G. G. Ryzhikh, J. Phys. B **35**, R81 (2002).
[21] J. Mitroy and M. W. J. Bromley, Phys. Rev. A **73**, 052712 (2006).
[22] M. W. J. Bromley and J. Mitroy, Int. J. Quantum Chem. **107**, 1150 (2007).
[23] J. Mitroy and G. G. Ryzhikh, J. Phys. B **32**, 2831 (1999); V. A. Dzuba *et al.*, Phys. Rev. A **60**, 3641 (1999).
[24] M. W. J. Bromley and J. Mitroy, Phys. Rev. Lett. **97**, 183402 (2006).
[25] Y. Nagashima *et al.*, Phys. Rev. B **58**, 12 676 (1998).
[26] L. C. Cota *et al.* (to be published).
[27] S. Takada *et al.*, Radiat. Phys. Chem. **58**, 781 (2000).
[28] R. Saniz *et al.*, Phys. Rev. Lett. **99**, 096101 (2007).
[29] A. Derevianko, B. Obreshkov, and V. A. Dzuba, Phys. Rev. Lett. **103**, 133201 (2009).
[30] R. H. Dicke, Phys. Rev. **89**, 472 (1953).
[31] For example, in a sample 100 nm thick with a residence time of only 1 ns, the average speed would be $\sim 10^4$ cm/s, giving a Doppler width of less than 0.0001 nm.